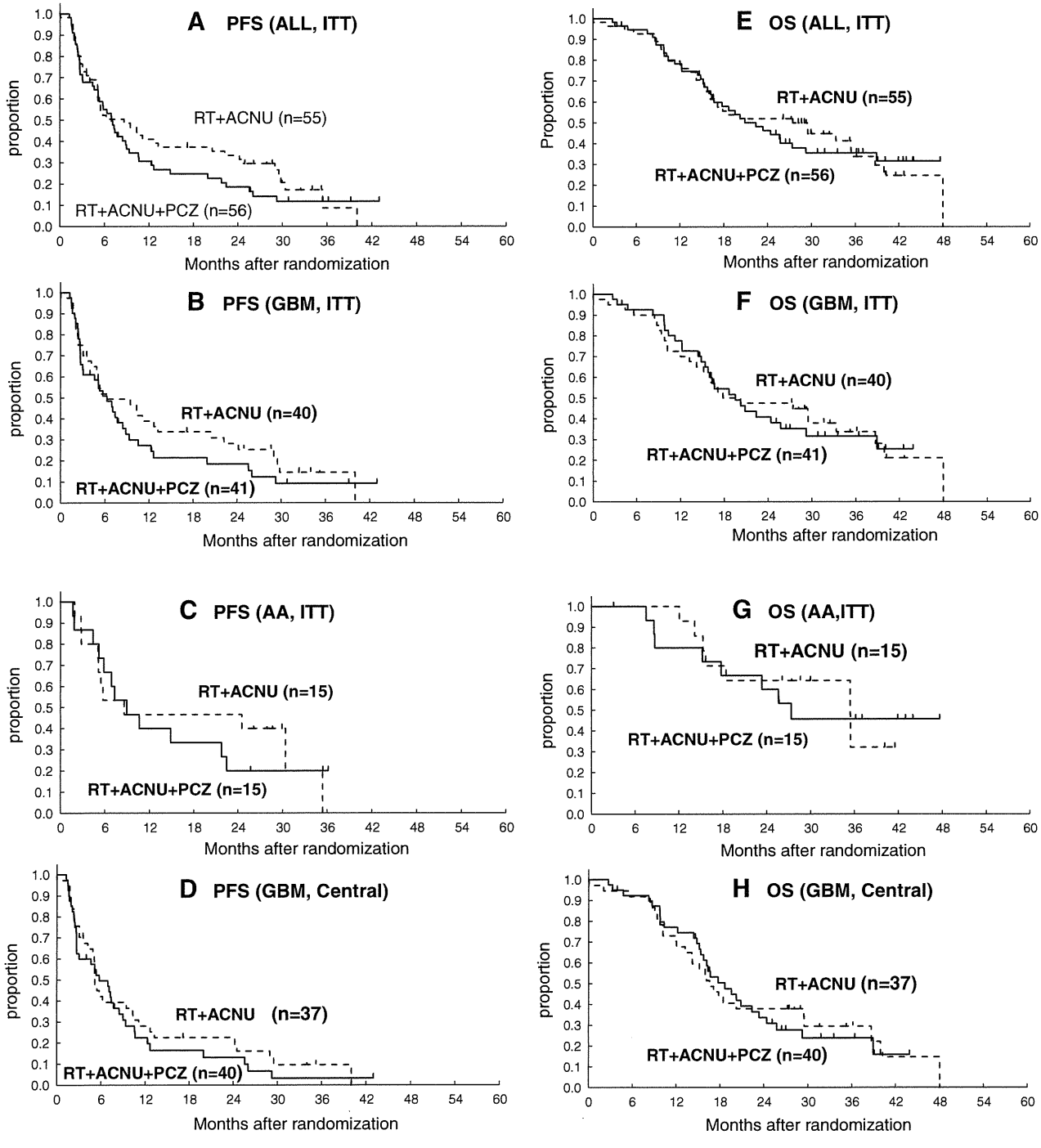

Fig. 2 Progression-free survival in the intention-to-treat (ITT) population (**a**), the GBM subgroup (**b**), the AA subgroup (**c**), and the GBM subgroup with central pathology review (**d**). Overall survival in the ITT population (**e**), the GBM subgroup (**f**), the AA subgroup (**g**), and the GBM subgroup with central pathology review (**h**). RT + ACNU alone (*solid line*), RT + ACNU + PCZ (*dotted line*)

Overall survival and cause of death

From the entire ITT population, 35 patients died in each group. In arm A ($n = 55$), OS was 27.4 months (95 % CI 16.2–35.4), compared with 22.4 months (95 % CI 16.4–29.2) in arm B ($n = 56$) (Fig. 2e). The %2-year survival in arms A and B was 51.9 % and 46.2 %, respectively. There was no difference between the 2 arms ($p = 0.75$ and pre-planned, one-sided $p = 0.62$, by stratified log-rank test).

The OS of GBM subgroup in arms A ($n = 40$, 28 death) and B ($n = 41$, 27 death) was 19.0 (95 % CI 15.2–33.3) and 19.5 months (95 % CI 15.8–29.2), respectively ($p = 0.90$) (Fig. 2f). The %2-year survival in arms A and B was 48 and 41 %, respectively. The OS of AA subgroup in arms A ($n = 15$, 7 death) and in arm B ($n = 15$, 8 death) was 35.4 [95 % CI 15.7–not estimated (NE)] and 27.4 months (95 % CI 17.8–NE), respectively ($p = 0.88$) (Fig. 2g). There were no differences between the arms of any subgroup.

In the subgroups defined by central pathology review, the OS of GBM in arm A ($n = 37$, 28 death) and in arm B ($n = 40$, 29 death) was 16.6 (95 % CI 13.3–29.5) and 18.7 months (95 % CI 15.4–23.4), respectively ($p = 0.92$) (Fig. 2h). The %2-year survival in arms A and B was 38 and 34 %, respectively. The OS of AA and AOA in arm A ($n = 9$, 3 death) and B ($n = 12$, 4 death) was 33.3 months (95 % CI 15.7–33.3) and NE, respectively ($p = 0.83$).

Among the 70 total deaths, 31/35 (88.6 %) patients in arm A and 32/35 (91.4 %) in arm B experienced neuronal death of an original tumor. One patient (2.9 %) in arm A and 2 (5.7 %) patients in arm B contracted treatment-related pneumonia and died from that illness. Other causes of death were pulmonary embolism (1), pneumonia (2), and unknown (1).

Toxicity

Toxicity was assessed in 110 patients receiving initial therapy and in 73 patients receiving adjuvant chemotherapy. The most frequent grade 3/4 toxicities, experienced by more than 10 % of patients, were hematologic, neurologic, gastrointestinal, and hepatic AEs (Table 4). Patients in both arms frequently experienced leukopenia and neutropenia; more than half of the patients in arm B experienced these AEs during adjuvant therapy as well as during initial therapy. More than 40 % of patients in arm A also experienced these hematologic events even during adjuvant therapy. Grade 4 neutropenia was observed in 5.6 and 39.3 % of patients in arms A and B during initial chemoradiotherapy and 11.1 and 15.6 % during adjuvant therapy. Grade 3/4 nausea and anorexia were seen in 10.7 and 16.1 % of patients in initial therapy in arm B, but were rare in the adjuvant-therapy subgroups in both arms. One patient in arm B had cerebral infarction. Extrapyramidal signs, including tremors or involuntary movements, occurred in 2 patients in each arm.

Grade 3/4 pneumonitis occurred in 1 patient in arm A and 2 in arm B during the entire treatment period. Opportunistic infections—including 2 cases of *Pneumocystis jirovecii* pneumonia (PCP), 1 case of oral candidiasis, and 2 case of herpes zoster—occurred in arm B. One patient (1.8 %) in arm A and 2 (3.6 %) patients in arm B died from treatment-related pneumonia, and 1 of these patients in arm B had PCP. One patient in arm B died from sepsis and acute respiratory distress syndrome after initial therapy. One patient in arm A died from pulmonary embolism before starting chemoradiotherapy, and 1 patient in arm A and 2 patients in arm B died from pneumonia following tumor progression.

Radiation necrosis was observed in 2 out of 54 (3.7 %) patients in arm A and 1 out of 56 (1.8 %) patients in arm B. During surgery, 1 patient in arm A was found to have radiation necrosis. Pseudo-progression within 3 months after chemoradiotherapy was not suspected in any patient.

Discussion

This study aimed to evaluate the efficacy and safety of treatment with ACNU + PCZ compared to ACNU alone as concomitant chemoradiotherapy against AA and GBM. We found no obvious differences in OS or PFS for AA and GBM between the treatment groups, but patients treated with ACNU + PCZ experienced more adverse effects than those treated with ACNU alone. TMZ is an effective regimen for malignant gliomas with less toxicity than our ACNU regimens, but it was not approved in Japan when this study began. At the end of the phase II part of this study, TMZ became available even in Japan, so this study was terminated at that point.

Methylguanine DNA methyltransferase is a major DNA repair protein and is implicated in resistance of glioma cells to alkylating agents [13]. Transcriptional silencing by MGMT promoter methylation results in inhibition of MGMT expression [14], and thus MGMT promoter methylation is strongly associated with survival in glioma patients treated with either nitrosourea or TMZ [15–17]. The status of the promoter of MGMT in primary tumors was frequently observed to change from methylated to unmethylated in recurrent tumors following ACNU or TMZ treatment [18, 19], which constitutes one of the mechanisms behind malignant gliomas' resistance to nitrosourea and TMZ. The rationale for treatment with ACNU + PCZ is that daily application of PCZ depletes MGMT activity, increasing sensitivity of AA and GBM to ACNU. Dose-dense TMZ therapy based on the theory of depletion of MGMT [20, 21], or BCNU or TMZ with direct inhibition of MGMT by O^6-benzylguanine [22, 23] has been shown in previous studies to be effective for GBMs. However, there was no difference in OS found between standard and dose-dense TMZ for newly diagnosed GBMs [20].

While we were conducting this study, the European Organization for Research and Treatment of Cancer (EORTC) Brain Tumor and Radiotherapy Groups and the

Table 4 Toxicity

Grade 3/4 adverse events	Initial therapy with RT ($n = 110$) (%)		Adjuvant therapy ($n = 73$) (%)	
	Arm A	Arm B	Arm A	Arm B
Hematologic				
Leukopenia	38.9	73.2	40.5	69.4
Neutropenia	38.9	76.8	44.4	56.3
Thrombocytopenia	5.6	50.0	40.5	50.0
Anemia	0	8.9	10.8	8.3
Neurologic				
Seizure	9.3	7.1	5.4	8.8
Speech impairment	11.1	10.7	5.4	2.9
Neuropathy-motor	11.1	12.5	0	0
Extrapyramidal sign	0	0	5.4	2.7
Pulmonary (pneumonitis)	0	3.6	2.7	0
Gastrointestinal				
Nausea	0	10.7	0	0
Anorexia	1.9	16.1	0	2.9
Hepatic				
AST	3.7	12.5	2.9	2.9
ALT	3.7	16.1	2.9	8.8
Total bilirubin	1.9	5.4	0	0
Renal (creatinine)	0	0	0	0
Metabolic				
Hyponatremia	1.9	8.9	5.9	2.9
Hypokalemia	1.9	7.1	2.9	2.9
Fever	0	3.6	0	0
Dermatologic: erythema	3.7	5.4	0	2.9

National Cancer Institute of Canada (NCIC) Clinical Trials Group (EORTC/NCIC TMZ study) reported, in 2005, that RT + TMZ significantly prolonged the survival of GBM patients compared to RT alone [24]. The median PFS, OS, and 2-year survival for RT + TMZ were 6.9, 14.6 months, and 26.5 %, respectively [24]. Although our results compared favorably with the EORTC/NCIC TMZ study, the PFS of RT + ACNU alone for GBMs in our ITT population and in GBM subgroups in central pathology review were 6.2 and 5.1 months, shorter than those from the EORTC/NCIC TMZ study. Since more than half of the patients in our study underwent TMZ treatment following disease progression, it is possible that TMZ rescued these patients with progression after ACNU regimens and prolonged the survival of these patients.

The incidence of grade 3/4 hematologic AEs—such as leukopenia, neutropenia, and thrombocytopenia—were reported to be 5, 4, and 11 %, respectively, in adjuvant TMZ therapy in the EORTC/NCIC TMZ trial [24]. Compared to TMZ, even ACNU alone caused severe hematologic AEs in 40 % of the patients in our study, and most of those patients in both arms discontinued the treatment protocol due to AEs or patient refusal related to AEs. It is noteworthy that approximately 30 % of patients in both arms failed to start adjuvant chemotherapy. The low completion rate of our protocol might explain the lack of differences in PFS and OS between the arms. After 2 patients in arm B experienced PCP, prophylactic use of cotrimoxazole (trimethoprim–sulfamethoxazole) against PCP was recommended in this study and was found to be useful.

Radiation necrosis has been reported in 2.5–21 % of patients undergoing chemoradiotherapy against malignant gliomas [25]. This complication was observed in 2.7 % of the patients in our study, but was tolerable. "Pseudo-progression" is the phenomenon of transient early disease progression after treatment with chemoradiotherapy consisting of TMZ for GBM progressive and enhancing lesions, as shown on MRI images taken immediately after treatment [25]. No patients in our study were suspected of pseudo-progression within 6 months after beginning chemoradiotherapy.

In general, the difference in histological diagnosis for local versus central pathology review is a major problem in the conduct of clinical trials on gliomas [26]. In our study, the concordance of GBM and AA between local and central diagnosis was low, but nearly identical to previous reports. In the EORTC/NCIC TMZ trial, central pathology review was performed in 85 % of cases, which confirmed the diagnosis of GBM in 93 % of the reviewed cases; 3 % had AA or AOA. In the phase III study of RT versus RT + BCNU + dibromodulcitol (EORTC 26882), of the 193 cases of AA diagnosed by the local pathologist, 176 were reviewed by the central pathologist. At review, 61 patients (35 %) were diagnosed with AA, 13 (8 %) with AOA, 4 (2 %) with AO, 44 (25 %) with GBM, 41 (23 %) with low-grade gliomas, and 13 (7 %) with another diagnosis [27].

The WHO classification system reflects the prognoses depending on grade I–IV tumors, or astrocytic or oligodendroglial tumors. However, it is based on morphological descriptions and contains subjective elements; thus, inter-observer variation occurs. The boundaries between grades II, III, and IV in gliomas are unclear, and there is a trend toward a more frequent diagnosis of oligodendroglial tumors [28]. Central pathological review before inclusion of a patient into clinical study is ideal, but it is very difficult to complete for aggressive grade III/IV tumors. Even if central review before enrollment is difficult in a multi-institutional setting, it is indispensable to perform post hoc central review at least in order to appropriately interpret the results of clinical studies of gliomas. A consensus meeting might also be useful before commencing clinical studies in order to gain concordance between local and central diagnoses. More objective classification of tumors based on

genotype, such the IDH1/2 mutation or 1p/19q codeletion, should be included in at least the stratification factor and subgroup analysis.

Conclusions

No significant differences in OS or PFS were found between ACNU alone and ACNU + PCZ in either AA or GBM. We found that ACNU + PCZ treatment was more toxic in our treatment schedule. Therefore, we conclude that the addition of PCZ to ACNU was not beneficial for newly diagnosed, high-grade astrocytomas as compared to ACNU alone. Considering the greater number of AEs associated with ACNU regimens, RT + TMZ should serve as a standard therapeutic regimen in the treatment of newly diagnosed AA and GBM.

Acknowledgments We thank all the members of the JCOG Brain Tumor Study Group and the staff of the JCOG Data Center. We appreciate Dr. Nobuaki Funata and Dr. Toru Iwaki for pathological review, Dr. Satoshi Ishikura for quality assurance of radiation therapy, and Dr. Hiroshi Katayama, Dr. Kenichi Nakamura, and Mr. Hidenobu Yamada for review of the manuscript. This work was supported in part by the National Cancer Center Research and Development Fund (23A-16 and 23A-20), the Health and Labour Sciences Research Grants (H14-032, H15-025, H16-005, H17-005), and the Grant-in Aid for Cancer Research (20S-4, 20S-6) from the Ministry of Health, Labour and Welfare.

Conflict of interest The authors declare that they have no conflict of interest.

References

1. The Committee of Brain Tumor Registry of Japan (2003) Report of brain tumor registry of japan (1984–2000) 12th edition. Neurol Med Chir (Tokyo) 49(Suppl):1–101
2. Glioma Meta-analysis Trialists (GMT) Group (2002) Chemotherapy in adult high-grade glioma: a systematic review and meta-analysis of individual patient data from 12 randomised trials. Lancet 359(9311):1011–1018. doi:10.1016/S0140-6736(02)08091-1
3. Matsutani M, Nakamura O, Nakamura M, Nagashima T, Asai A, Fujimaki T, Tanaka H, Ueki K, Tanaka Y (1994) Radiation therapy combined with radiosensitizing agents for cerebral glioblastoma in adults. J Neurooncol 19(3):227–237
4. Wolff JE, Berrak S, Koontz Webb SE, Zhang M (2008) Nitrosourea efficacy in high-grade glioma: a survival gain analysis summarizing 504 cohorts with 24193 patients. J Neurooncol 88(1):57–63. doi:10.1007/s11060-008-9533-5
5. Takakura K, Abe H, Tanaka R, Kitamura K, Miwa T, Takeuchi K, Yamamoto S, Kageyama N, Handa H, Mogami H et al (1986) Effects of ACNU and radiotherapy on malignant glioma. J Neurosurg 64(1):53–57. doi:10.3171/jns.1986.64.1.0053
6. Pegg AE (1990) Mammalian O^6-alkylguanine-DNA alkyltransferase: regulation and importance in response to alkylating carcinogenic and therapeutic agents. Cancer Res 50(19):6119–6129
7. Silber JR, Bobola MS, Ghatan S, Blank A, Kolstoe DD, Berger MS (1998) O^6-methylguanine-DNA methyltransferase activity in adult gliomas: relation to patient and tumor characteristics. Cancer Res 58(5):1068–1073
8. Valavanis C, Souliotis VL, Kyrtopoulos SA (1994) Differential effects of procarbazine and methylnitrosourea on the accumulation of O^6-methylguanine and the depletion and recovery of O^6-alkylguanine-DNA alkyltransferase in rat tissues. Carcinogenesis 15(8):1681–1688
9. Souliotis VL, Kaila S, Boussiotis VA, Pangalis GA, Kyrtopoulos SA (1990) Accumulation of O^6-methylguanine in human blood leukocyte DNA during exposure to procarbazine and its relationships with dose and repair. Cancer Res 50(9):2759–2764
10. Wedge SR, Porteus JK, May BL, Newlands ES (1996) Potentiation of temozolomide and BCNU cytotoxicity by O(6)-benzylguanine: a comparative study in vitro. Br J Cancer 73(4):482–490
11. Therasse P, Arbuck SG, Eisenhauer EA, Wanders J, Kaplan RS, Rubinstein L, Verweij J, Van Glabbeke M, van Oosterom AT, Christian MC, Gwyther SG (2000) New guidelines to evaluate the response to treatment in solid tumors. European Organization for Research and Treatment of Cancer, National Cancer Institute of the United States, National Cancer Institute of Canada. J Natl Cancer Inst 92(3):205–216
12. Bernstein D, Lagakos SW (1978) Sample size and power determination for stratified clinical trials. J Stat Comput Simul 8:65–73
13. Bobola MS, Tseng SH, Blank A, Berger MS, Silber JR (1996) Role of O^6-methylguanine-DNA methyltransferase in resistance of human brain tumor cell lines to the clinically relevant methylating agents temozolomide and streptozotocin. Clin Cancer Res 2(4):735–741
14. Esteller M, Garcia-Foncillas J, Andion E, Goodman SN, Hidalgo OF, Vanaclocha V, Baylin SB, Herman JG (2000) Inactivation of the DNA-repair gene MGMT and the clinical response of gliomas to alkylating agents. N Engl J Med 343(19):1350–1354. doi:10.1056/NEJM200011093431901
15. Hegi ME, Diserens AC, Gorlia T, Hamou MF, de Tribolet N, Weller M, Kros JM, Hainfellner JA, Mason W, Mariani L, Bromberg JE, Hau P, Mirimanoff RO, Cairncross JG, Janzer RC, Stupp R (2005) MGMT gene silencing and benefit from temozolomide in glioblastoma. N Engl J Med 352(10):997–1003. doi:10.1056/NEJMoa043331
16. Sonoda Y, Yokosawa M, Saito R, Kanamori M, Yamashita Y, Kumabe T, Watanabe M, Tominaga T (2010) O(6)-Methylguanine DNA methyltransferase determined by promoter hypermethylation and immunohistochemical expression is correlated with progression-free survival in patients with glioblastoma. Int J Clin Oncol 15(4):352–358. doi:10.1007/s10147-010-0065-6
17. van den Bent MJ, Gravendeel LA, Gorlia T, Kros JM, Lapre L, Wesseling P, Teepen JL, Idbaih A, Sanson M, Smitt PA, French PJ (2011) A hypermethylated phenotype is a better predictor of survival than MGMT methylation in anaplastic oligodendroglial brain tumors: a report from EORTC study 26951. Clin Cancer Res 17(22):7148–7155. doi:10.1158/1078-0432.CCR-11-1274
18. Brandes AA, Franceschi E, Tosoni A, Bartolini S, Bacci A, Agati R, Ghimenton C, Turazzi S, Talacchi A, Skrap M, Marucci G, Volpin L, Morandi L, Pizzolitto S, Gardiman M, Andreoli A, Calbucci F, Ermani M (2010) O(6)-methylguanine DNA-methyltransferase methylation status can change between first surgery for newly diagnosed glioblastoma and second surgery for recurrence: clinical implications. Neuro Oncol 12(3):283–288. doi:10.1093/neuonc/nop050
19. Okita Y, Narita Y, Miyakita Y, Ohno M, Fukushima S, Kayama T, Shibui S (2012) Pathological findings and prognostic factors in recurrent glioblastomas. Brain Tumor Pathol. doi:10.1007/s10014-012-0084-2
20. Aldape KD, Wang M, Sulman EP, Hegi M, Colman H, Jones G, Chakravarti A, Mehta MP, Andrews DW, Long L, Diefes K,

Heathcock L, Jenkins R, Schultz CJ, Gilbert MR, Group RTO (2011) RTOG 0525: Molecular correlates from a randomized phase III trial of newly diagnosed glioblastoma. ASCO Annu Meet Proc 29(18_suppl):LBA2000

21. Wick A, Felsberg J, Steinbach JP, Herrlinger U, Platten M, Blaschke B, Meyermann R, Reifenberger G, Weller M, Wick W (2007) Efficacy and tolerability of temozolomide in an alternating weekly regimen in patients with recurrent glioma. J Clin Oncol 25(22):3357–3361. doi:10.1200/JCO.2007.10.7722
22. Quinn JA, Jiang SX, Reardon DA, Desjardins A, Vredenburgh JJ, Rich JN, Gururangan S, Friedman AH, Bigner DD, Sampson JH, McLendon RE, Herndon JE 2nd, Walker A, Friedman HS (2009) Phase II trial of temozolomide plus O^6-benzylguanine in adults with recurrent, temozolomide-resistant malignant glioma. J Clin Oncol 27(8):1262–1267. doi:10.1200/JCO.2008.18.8417
23. Quinn JA, Pluda J, Dolan ME, Delaney S, Kaplan R, Rich JN, Friedman AH, Reardon DA, Sampson JH, Colvin OM, Haglund MM, Pegg AE, Moschel RC, McLendon RE, Provenzale JM, Gururangan S, Tourt-Uhlig S, Herndon JE 2nd, Bigner DD, Friedman HS (2002) Phase II trial of carmustine plus O(6)-benzylguanine for patients with nitrosourea-resistant recurrent or progressive malignant glioma. J Clin Oncol 20(9):2277–2283
24. Stupp R, Mason WP, van den Bent MJ, Weller M, Fisher B, Taphoorn MJ, Belanger K, Brandes AA, Marosi C, Bogdahn U, Curschmann J, Janzer RC, Ludwin SK, Gorlia T, Allgeier A, Lacombe D, Cairncross JG, Eisenhauer E, Mirimanoff RO (2005) Radiotherapy plus concomitant and adjuvant temozolomide for glioblastoma. N Engl J Med 352(10):987–996
25. Brandes AA, Tosoni A, Spagnolli F, Frezza G, Leonardi M, Calbucci F, Franceschi E (2008) Disease progression or pseudoprogression after concomitant radiochemotherapy treatment: pitfalls in neurooncology. Neuro Oncol 10(3):361–367. doi:10.1215/15228517-2008-008
26. van den Bent MJ (2010) Interobserver variation of the histopathological diagnosis in clinical trials on glioma: a clinician's perspective. Acta Neuropathol 120(3):297–304. doi:10.1007/s00401-010-0725-7
27. Hildebrand J, Gorlia T, Kros JM, Afra D, Frenay M, Omuro A, Stupp R, Lacombe D, Allgeier A, van den Bent MJ (2008) Adjuvant dibromodulcitol and BCNU chemotherapy in anaplastic astrocytoma: results of a randomised European Organisation for Research and Treatment of Cancer phase III study (EORTC study 26882). Eur J Cancer 44(9):1210–1216. doi:10.1016/j.ejca.2007.12.005
28. Coons SW, Johnson PC, Scheithauer BW, Yates AJ, Pearl DK (1997) Improving diagnostic accuracy and interobserver concordance in the classification and grading of primary gliomas. Cancer 79(7):1381–1393

Brain Tumor Pathol (2011) 28:43–51
DOI 10.1007/s10014-010-0002-4

ORIGINAL ARTICLE

Precise comparison of protoporphyrin IX fluorescence spectra with pathological results for brain tumor tissue identification

Takehiro Ando · Etsuko Kobayashi · Hongen Liao · Takashi Maruyama · Yoshihiro Muragaki · Hiroshi Iseki · Osami Kubo · Ichiro Sakuma

Received: 3 March 2010 / Accepted: 13 July 2010 / Published online: 25 December 2010

Abstract Photodynamic diagnosis is used during glioma surgery. Although some studies have shown that the spectrum of fluorescence was efficient for precise tumor diagnosis, previous methods to characterize the spectrum have been problematic, which can lead to misdiagnosis. In this paper, we introduce a comparison technique to characterize spectrum from pathology and results of preliminary measurement using human brain tissues. We developed a spectrum scanning system that enables spectra measurement of raw tissues. Because tissue preparations retain the shape of the device holder, spectra can be compared precisely with pathological examination. As a preliminary analysis, we measured 13 sample tissues from five patients with brain tumors. The technique enabled us to measure spectra and compare them with pathological results. Some tissues exhibited a good relationship between spectra and pathological results. Although there were some false positive and false negative cases, false positive tissue had different spectra in which intensity of short-wavelength side was also high. The proposed technique provides an accurate comparison of quantitative fluorescence spectra with pathological results. We found that spectrum analysis may reduce false positive errors. These results will increase the accuracy of tumor tissue identification.

Keywords 5-Aminolevulinic acid · Protoporphyrin IX · Fluorescence spectra · Photodynamic diagnosis

T. Ando (✉) · E. Kobayashi · H. Liao · I. Sakuma
Department of Bioengineering, Graduate School of Engineering, The University of Tokyo, Engineering building No.14, Room 722, Hongo 7-3-1, Bunkyo, Tokyo 113-8656, Japan
e-mail: take_and_o@bmpe.t.u-tokyo.ac.jp

T. Maruyama · H. Iseki · O. Kubo
Department of Neurosurgery, Neurological Institute, Tokyo Women's Medical University, Shinjuku, Tokyo 162-8666, Japan

Y. Muragaki · H. Iseki
Institute of Advanced Biomedical Engineering and Science, Tokyo Women's Medical University, Shinjuku, Tokyo 162-8666, Japan

Introduction

Over recent decades, photodynamic diagnosis (PDD) has been studied for intraoperative tumor diagnosis, especially glioma. PDD uses autofluorescence or endogenous fluorescence materials [1–4], and the technique can be easily applied for clinical practice because the system is simple. In a number of clinical studies, 5-aminolevulinic acid (5-ALA)-induced protoporphyrin IX (PpIX) fluorescence has been used for intraoperative tumor diagnosis. Although 5-ALA and PpIX are natural substances produced by the human body, orally administrated 5-ALA accumulates in tumor cells and is converted to PpIX by heme biosynthesis. Accumulation of 5-ALA in a tumor cell may be caused by a damaged blood brain barrier (BBB) or iron (Fe)-metabolic enzyme defect, such as ferrochelatase [5]. However, the exact mechanism is still unknown.

Stummer et al. [1–3] introduced the use of the fluorescence surgical microscope to examine PpIX fluorescence for intraoperative tumor detection. They reported that some regions of brain and tumor tissue have different fluorescence characteristics (intensity and color) and assessed these tissues pathologically. Although this approach was appropriate for fluorescence-guided surgery, fluorescence measurement was not quantitative. A recent study of quantitative fluorescence measurement showed that PpIX spectrum shape is important to precisely detect tumor and

diagnose malignancy [6]. Another group reported that ultraviolet (UV) laser and white light reveal differences in the autofluorescence spectra between tumor and normal brain tissue [7, 8]. Although these quantitative studies found characteristic tumor tissue spectra when comparing them with pathological results, the comparison methods used have the following limitations. First, there is a possibility that a spectrum measurement point is different from a pathology examination point. This means that a spectrum characterization may not be correct. Second, because the spectrum measurement was performed after staining or fixation with formalin, the measured spectrum may be different from that of the raw tissue. To use the result in situ, raw tissue spectrum measurement is necessary. Finally, although tumor margin characterization is necessary for precise resection, these methods cannot determine spatial changes in spectra.

To solve these problems, we developed a spectrum scanning system that enables acquisition of raw tissue spectra distribution. Furthermore, our novel protocol makes it possible to precisely compare spectra with pathological results. In this paper, we introduce the technique we devised and present results of preliminary measurements.

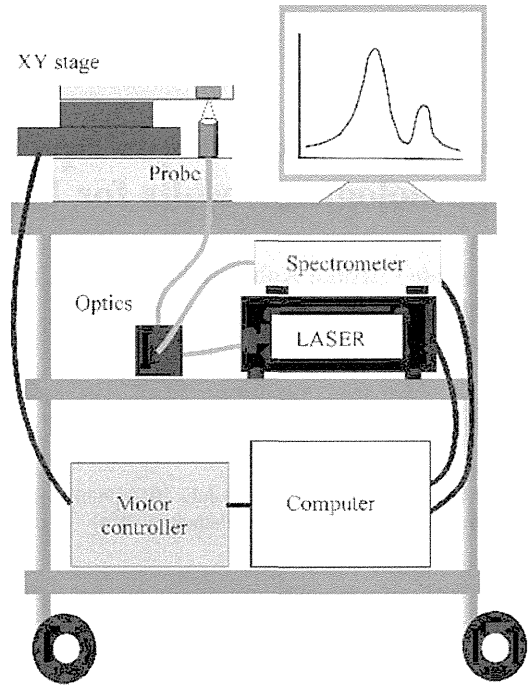

Fig. 1 Overall view of the measurement system

Materials and methods

Measurement system

A spectrum-scanning system for 5-ALA-induced PpIX fluorescence was especially designed for both fluorescence measurement and fluorescence spectra comparison with pathological results. The system consists of an excitation laser (VLS405-SA3, Digital Stream), a spectrometer (WTC-111E B&W, TEK Inc.), optics, and a computer (Fig. 1). The excitation laser emits 405 nm of UV light, and the maximal output power is 15 mW. The spectrometer wavelength range is 300–850 nm. The measurement probe uses a coaxial optical system. All light paths are connected with optical fibers (core diameter 365 μm, multimode), and a dichroic mirror is used to separate excitation light and fluorescence. To insert a dichroic mirror in the light path, three collimator lenses are mounted to a cubic box. Angles and positions of all collimator lenses and the dichroic mirror angle can be adjusted to improve the coupling efficiency of the light. It is also equipped with a long-pass filter to separate strong reflected excitation light from the fluorescence signal. There are two achromatic lenses at the tip of the probe. The focal length of the fiber side lens is 19 mm, the object side is 30 mm, the working distance is 21.7 mm, and the lens diameter is 12.5 mm. The measurement spot diameter is evaluated using a phantom, the optical character of which is designed to match that of brain tissue. As a result, the system's measuring diameter is estimated as 0.8 mm.

To measure fluorescence spectra spatial changes, the measurement probe is fixed under an *XY* stage (SGSP20-35XY, Sigma Koki), and the sample tissues are then moved. A removable tissue holder that has a square 5-mm hole is set on the stage. One corner of the holder hole is cut down to make a shape mark. Because the holder location is registered to the *XY* stage coordinates, it is possible to follow the measuring position. In this study, spectra of 58 points were acquired from each sample tissue.

Measurement protocol

To accurately compare spectra with pathological results, we devised the following measurement protocol:

1. Resected tissue was gently put in the measurement system tissue holder.
2. The spectrum of each point was measured by the system, and data were processed automatically.
3. After measurement, the tissue and the holder were put in liquid nitrogen to freeze the tissue.
4. The frozen tissue was taken out of the holder and sectioned using conventional methods.
5. The sectioned tissue was stained with hematoxylin–eosin (H&E).

Sectioning and staining were performed by a pathologist. Spectrometer exposure time and the laser power were

arbitrarily adjusted depending on each patient. Although this protocol is relatively complicated, because the frozen tissue retains the original shape of the holder and the measured surface can be maintained, it is possible to make a "holder-shaped" histological preparation. This preparation makes it possible to compare cell characteristics with the corresponding measurement points from the tissue shape and the *XY*-stage coordinates. Furthermore, because the spectrum is measured before freezing or staining, this method allows the use of raw brain tissue spectra for comparison. This means that the results can be directly applied to intraoperative measurement and resection.

Data processing

Because measured spectra contain some noise, data were smoothed using the Savitzky–Golay method (25-point smoothing) [9]. After smoothing, spectra data were processed to extract each PpIX peak intensity and wavelength from raw data, which contain autofluorescence spectra. The procedure is as follows: First, we empirically approximated a curve of a background autofluorescence spectrum as a quartic function using the least mean squares (LMS) method. To draw the LMS curve, data sets of 590–610 and 747–913 nm were used (Fig. 2). After LMS curve (background) subtraction from raw data, PpIX peak intensity and wavelength were calculated as maximal intensity and its wavelength. We recorded not only the PpIX intensity but also intensity at 585 nm, which represents the intensity of short-wavelength side. These data were plotted on a contour map.

Ex vivo measurement and pathological examination

Using the system we developed, we measured brain tissues resected during brain tumor operations at Tokyo Women's Medical University Hospital. At 7:30 a.m. on the day of the operation, 5-ALA at a dosage of 20 mg/kg body weight was orally administered to patients who were suspected of having a glioma. We targeted primary gliomas in five patients whose magnetic resonance image MRI results suggested that the tumors were grade III or IV. Measurement was performed at about 2:00 p.m. on the same day. Preparations for pathological examinations were made using the method mentioned earlier. Spectrometer exposure time was arbitrary set to 70–500 ms for each measurement point. Measurement time, including processing time, was approximately 10–40 s for each sample tissue. The pathological examinations were performed by a pathologist, and examiners were blinded to fluorescence measurement. All experimental protocols were approved by the Ethical Committee of Tokyo Women's Medical University.

Results

Tumor types of each patient in this study were as follows:

Case 1: Glioblastoma multiforme (GBM)
Case 2: Anaplastic oligodendro-astrocytoma (AOA)
Case 3: Anaplastic oligodendroglioma (AO)
Case 4: Oligodendroglioma (O)
Case 5: GBM

We obtained one tissue from case 1, four from case 2, three from case 3, one from case 4, and four from case 5. Each tissue is represented by a number (case number) and alphabetic letters. Figures 3–5 show examples of the results of tissue0 2D, 5A, and 5D, respectively. In 2D (Fig. 3a), a tumor margin is visible from which the tumor spread gradually from the upper to the lower side; intensity distribution of PpIX corresponded to its tumor distribution (Fig. 3b). Interestingly, intensity at 585 nm was in the

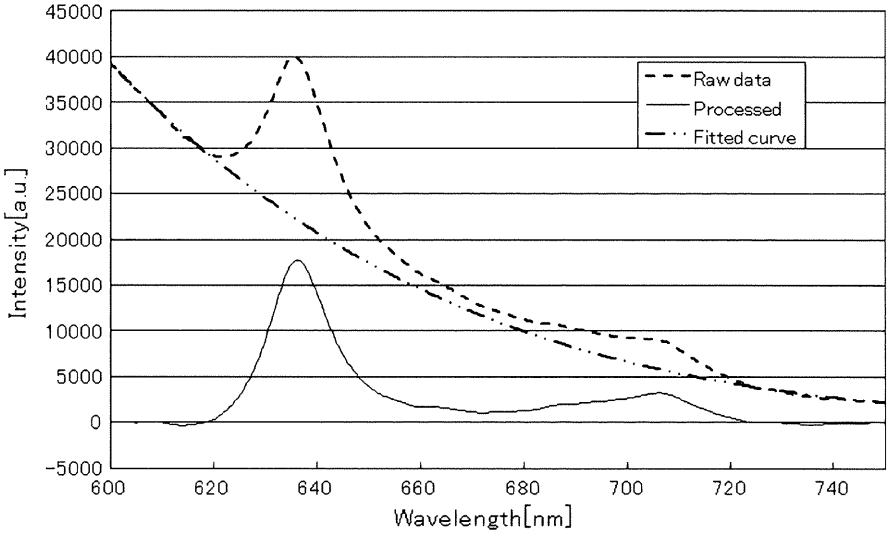

Fig. 2 Background subtraction. *Fitted curve* baseline plotted by the approximate curve of a quartic function. *Raw data* raw spectrum acquired from a specimen. *Processed* processed spectrum plotted by subtracting the base curve from the raw spectrum

opposite distribution (Fig. 3c), which means that the intensity was higher in the normal area (585 nm was determined from the property of a long-pass filter and represents intensity of the short-wavelength side). The peak wavelength seemed almost the same throughout the region (Fig. 3d).

Although tissue 5A had no tumorous cells and seemed to be the region close to the cortex, the tissue had evidence of angiogenesis and gliosis, which can be identified by increased reactive astrocytes (Fig. 4a). Although the tissue was not a tumor, PpIX intensity was as high as that of tumor fluorescence throughout the entire region (Fig. 4b). Therefore, this was a false positive case of fluorescence measurement. However, the 585 nm intensity (Fig. 4c) was higher than that found in other tumor tissues from the same patient. The peak wavelength seemed the same throughout the region (the center region in Fig. 4d shows the error data caused by spectrometer saturation. Because the PpIX spectrum was saturated, the peak wavelength could not be calculated). Tissue 5D was from a tumor margin that had local accumulation of tumor cells (Fig. 5a). PpIX intensity distribution was well correlated with pathological results (Fig. 5b). The intensity of 585 nm had the opposite distribution to PpIX fluorescence (Fig. 5c). Furthermore, the peak wavelength also had a similar distribution (it shifted to the short side at the nontumor region) (Fig. 5d).

Tissue 1 was a tumor margin; the left side was tumor area and the right side the cortex. There was a blood vessel visible at the bottom left corner of the image that emitted strong PpIX fluorescence. However, the intensity at 585 nm was low in the vessel area but high around the vessel. Tissues 2A and 2C showed tumors all over the region, and PpIX intensity was high. Although pathological results showed that tissue 2A was homogeneously tumorous, varied PpIX intensity was observed. Tissue 2C had many vessels on the upper side, and PpIX intensity was relatively high in the region. Tissue 2B was tumorous over the entire tissue area, but only a small portion emitted PpIX fluorescence. Tissue 3A had a tumorous area, but PpIX intensity distribution did not exactly correspond to its tumor area. However, the intensity distribution of 585 nm, which has an opposite distribution to PpIX, was similar to pathological results. Although tissue 3B was not a tumor with blood vessels, PpIX spectrum or any other characteristic spectra were not acquired. Tissue 3C was not tumorous, and PpIX fluorescence was not acquired. Although tissue 4 was tumorous, with tumor cells distributed throughout the entire area, PpIX fluorescence could not be detected over the entire region. Tissue 5B had a nonuniform tumor distribution, including cell characteristics implicating necrosis. This sample might be close to the center of the tumor. PpIX intensity was also nonuniform but showed low intensity around the necrotic area. Tissue 5C was tumor tissue that had diffused astrocytoma cells. PpIX intensity was high over the entire region.

Discussion

In this study, we introduced a novel technique to compare fluorescence spectra distribution of raw tissues with pathological results. We could confirm the necessity of a precise comparison because pathological results showed that cell characteristics varied with location, even when cell size was 5 × 5 mm, as in tissues 2D and 5D. Although we measured only 13 samples in this study, our comparisons showed some trends between spectra and pathological results, which can be divided into three groups. The first group had good correlation between spectra and pathological results, such as in tissues 2D and 5D. Furthermore, three tissues exhibited a relationship between pathological results and intensity distributions at 585 nm and PpIX peak wavelength. As noted earlier, intensity at 585 nm, which represents intensity of the short-wavelength side, has the opposite distribution to PpIX fluorescence. This light may come from an autofluorescence substance such as nicotinamide adenine dinucleotide (NADH), flavin, or lipofuscin [10]. In this study, considering excitation laser wavelength and emission spectrum, lipofuscin and flavin are anticipated to be the autofluorescence substances [11, 12]. Lipofuscin, in particular, appears in neuronal cells of aged patients and exhibits strong fluorescence, with a peak wavelength of approximately 560 nm. These results showed that the precise comparison of spectra with pathological results may increase diagnostic accuracy.

Some specimens, such as tissues 1 and 2C, exhibited high PpIX intensity around blood vessels. Because PpIX accumulates at tumor cells because of BBB disruption, PpIX is thought not to accumulate inside blood vessels. Although the high intensity of PpIX fluorescence was acquired at the blood vessel in tissue 1, the result was thought to be caused by infiltrating tumor around the blood vessel. Unfortunately, in this case, H&E preparation could not reveal the existence of infiltrating tumor cells because the measured point was very local, and preparation fixation was not optimum. In the case of tissue 2C, PpIX fluorescence intensity was relatively high around blood vessels. This result may demonstrate increased 5-ALA intake around blood vessels in which BBB are disrupted, which leads to considerable PpIX accumulation. Although we cannot show conclusive cause, tissue that has blood vessels should be investigated carefully.

The second group comprised false negative cases or cases in which fluorescence distribution was not correlated with pathological findings, such as tissues 2B and 4. There

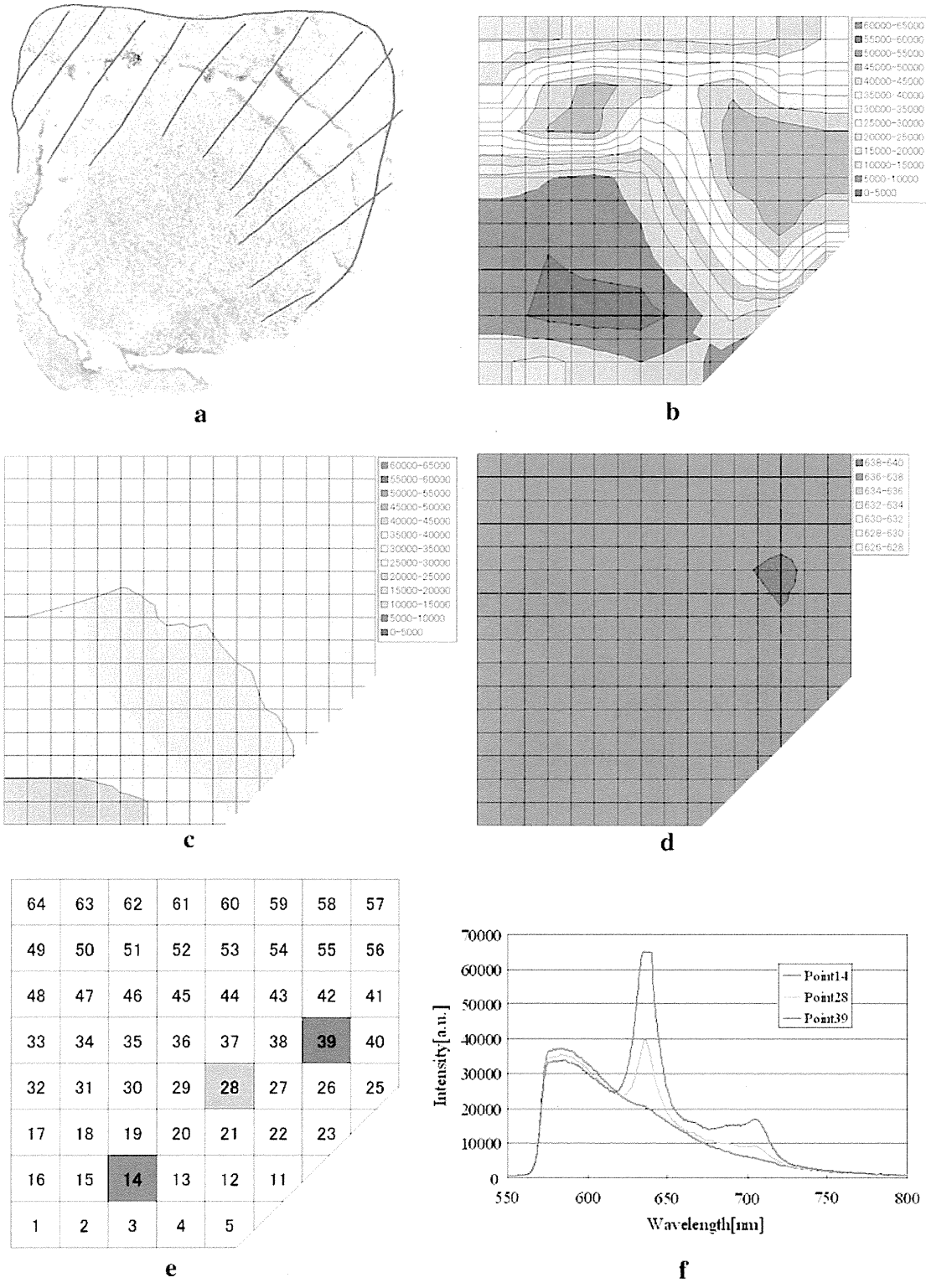

Fig. 3 Results for tissue 2D. **a** Pathological result: this tissue seemed to be the tumor margin. **b** Intensity distribution of protoporphyrin IX (PpIX) fluorescence. **c** Intensity distribution at 585 nm. **d** Peak wavelength distribution of PpIX fluorescence. **e** Examples of measured points. **f** Example of measured spectra corresponding to measured points (**e**)

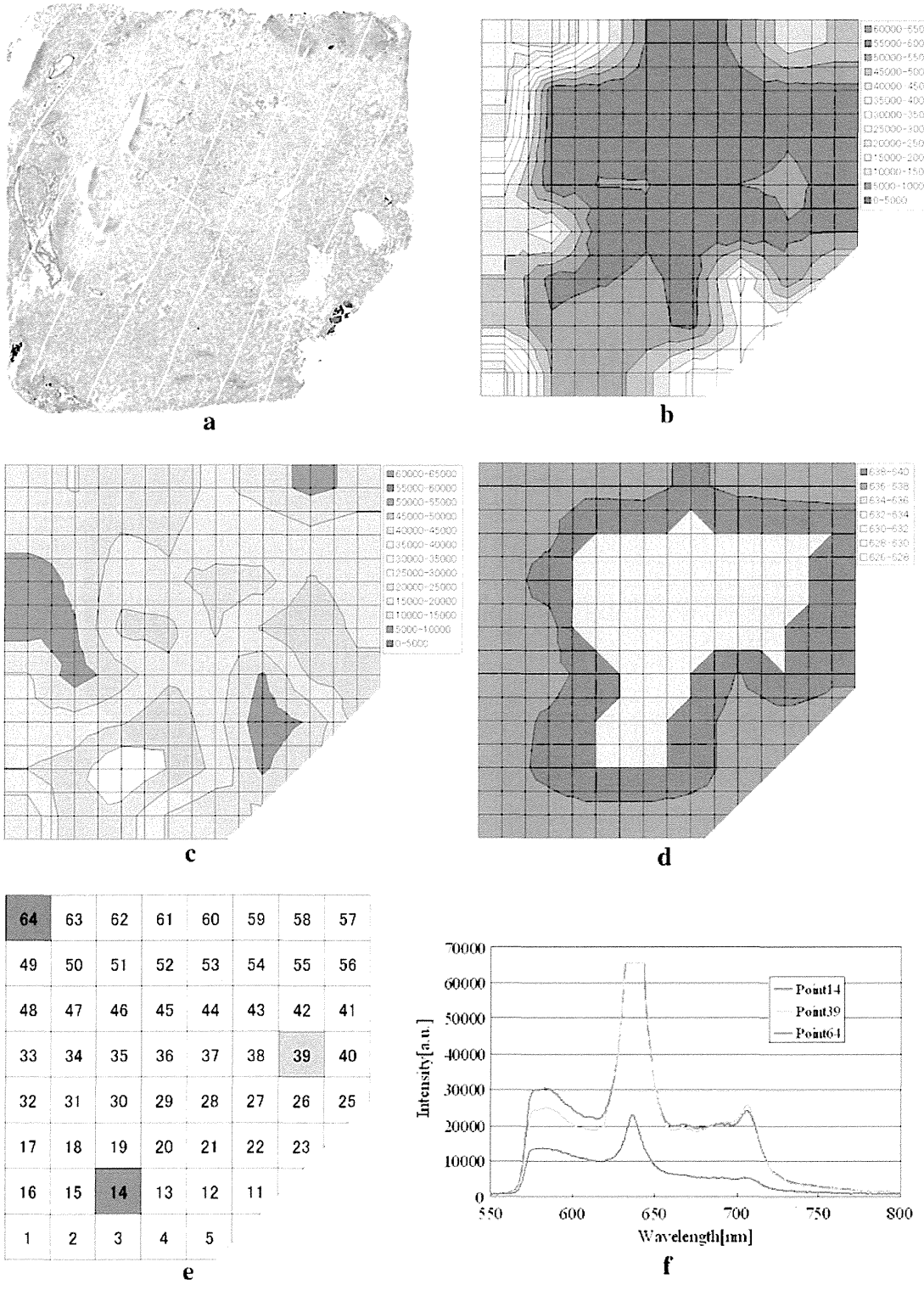

Fig. 4 Results for tissue 5A. **a** Pathological result: this tissue was not tumorous but included reactive astrocytes. **b** Intensity distribution of protoporphyrin IX (PpIX) fluorescence. **c** Intensity distribution at 585 nm. **d** Peak wavelength of distribution of PpIX fluorescence. **e** Examples of measured points. **f** Example of measured spectra corresponding to measured points (**e**)

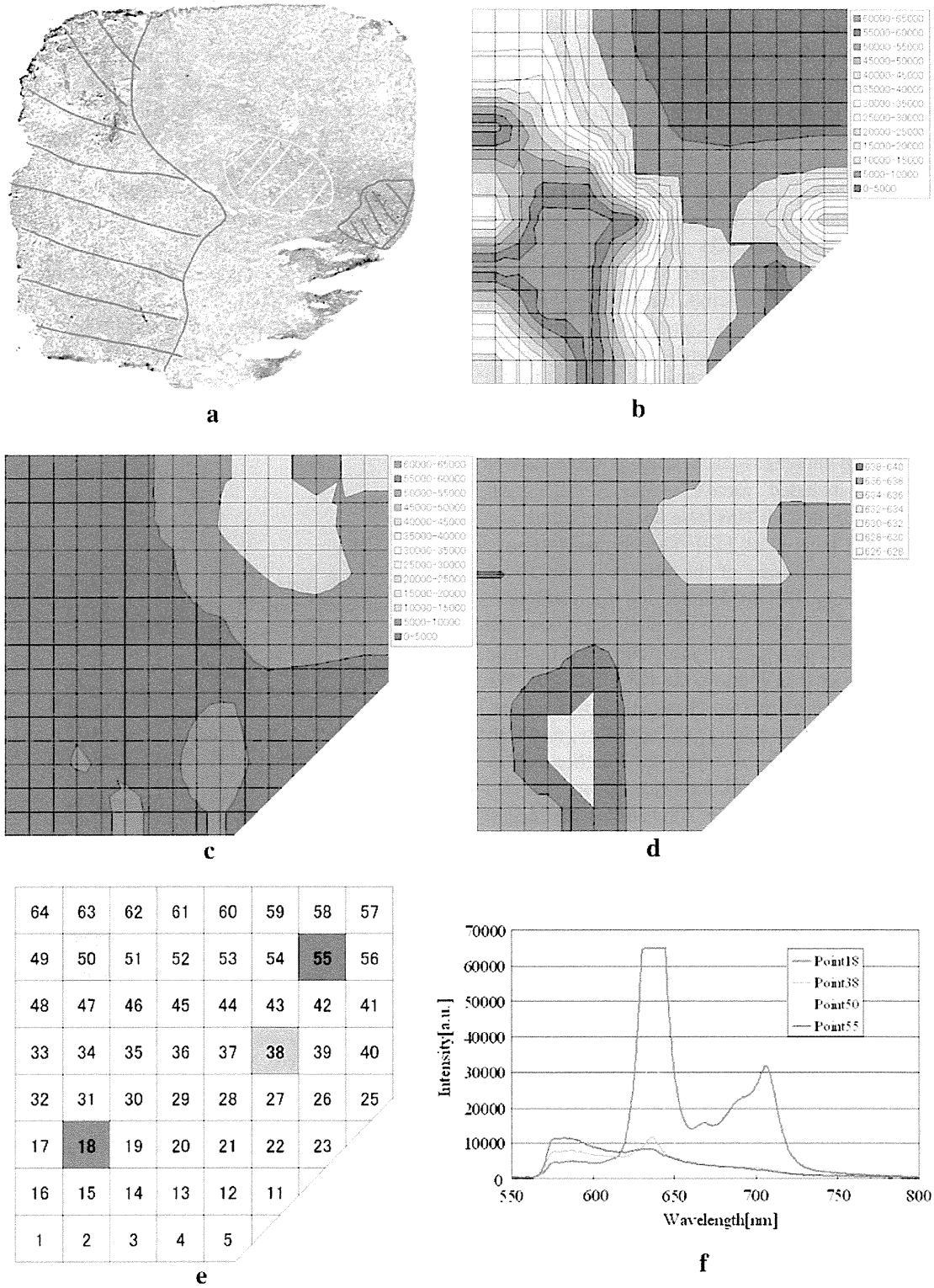

Fig. 5 Results of tissue 5D. **a** Pathological result: this tissue had characteristic tumor distribution (*blue line*) and reactive astrocytes (*yellow line*). **b** Intensity distribution of protoporphyrin IX (PpIX) fluorescence. **c** Intensity distribution at 585 nm. **d** Peak wavelength distribution of PpIX fluorescence. **e** Examples of measured points. **f** Example of measured spectra corresponding to measured points (**e**)

are two possible causes. First, adherent blood on the tissue surface may prevent PpIX fluorescence measurement. Because red blood cells efficiently absorb UV light, which was used as the excitation laser, the light may not reach tissue PpIX [13–15]. In order to avoid damaging cells and changing there characteristics, we did not wash the tissue; however, as much excessive blood as possible had to be removed Second, not enough PpIX accumulated to emit fluorescence. The intake of 5-ALA may depend on the state of the BBB, and this influences the amount of PpIX. Because the BBB was not damaged severely in the low-grade tumor, PpIX may not emit fluorescence in such patients. Actually, tissue 4 was considered an oligodendroglioma, which is classified as grade II according to the World Health Organization classification [16]. Although we cannot control 5-ALA intake, our method can reveal limitations of 5-ALA-induced PpIX fluorescence.

The third group encompassed the false positive case of tissue 5A, which included reactive astrocytes that appear when brain tissue is injured. This false negative finding was also reported by Utsuki et al. [17]. The original astrocyte (not reactive), which is one of the glia cells, has many functions in the brain, such as maintaining brain structure, regulating ion concentration in the extracellular space, and supporting metabolic activity. The most important function of the astrocyte is that it controls the BBB [18, 19]. We hypothesized that the astrocytes changed their characteristics when they became reactive; subsequently, the BBB did not function efficiently, resulting in a higher 5-ALA intake. However, although PpIX fluorescence was detected as false positive, our measurement showed that the spectra of the tissue, including reactive astrocytes, were different from those of the tumor (short-wavelength intensity was high), which may reduce false positive error.

There are certain limitations to our technique. We deliberately changed the exposure time of the spectrometer because fluorescence intensity varied greatly with tissues and exceeded the dynamic range of the spectrometer. This problem prevents comparison among patients and results in an undesirable variety of data. However, the issue can be solved using exchangeable neutral-density filters and some estimation calculations. We developed a modified system that enables maintenance of the same measurement conditions for all patients, and now we measure tissues from various types of glioma using the modified system. Those data will show accurate tumor discrimination and the limitation of 5-ALA-induced PpIX fluorescence. Furthermore, we are working on a robotic system that uses 5-ALA-induced PpIX fluorescence for diagnosis and a midinfrared laser for tumor ablation [20]. The system allows intraoperative tumor identification and ultraprecise ablation. We expect that the method presented in this paper will provide a more accurate intraoperative diagnosis.

Conclusion

We developed a spectrum scanning system that enabled precise comparison of tissue fluorescence spectra with pathological examination. Using the system, we measured 13 brain tissues from five patients and compared fluorescence spectra with pathology. Results showed that there was good correlation between fluorescence distribution and pathological results in high-grade tumor, and there were also false negative and false positive cases. We found that the spectrum of the false positive case, which had reactive astrocytes, was different from tumor spectrum. The results may reduce false positive error and lead to more accurate tumor discrimination PpIX fluorescence.

Acknowledgment This work was supported in part by grant for Translational Systems Biology and Medicine Initiative (TSBMI) and Grant-in-Aid for JSPS Fellows.

References

1. Stummer W, Stepp H, Moller G et al (1998) Technical principles for protoporphyrin-IX-fluorescence guided microsurgical resection of malignant glioma tissue. Acta Neurochir (Wien) 140(10):995–1000
2. Stummer W, Novotny A, Stepp H et al (2000) Fluorescence-guided resection of glioblastoma multiforme by using 5-aminolevulinic acid-induced porphyrins: a prospective study in 52 consecutive patients. J Neurosurg 93(6):1003–1013
3. Stummer W, Pichlmeier U, Meinel T et al (2006) Fluorescence-guided surgery with 5-aminolevulinic acid for resection of malignant glioma: a randomised controlled multicentre phase III trial. Lancet Oncol 7(5):392–401
4. Chung YG, Schwartz JA, Gardner CM et al (1997) Diagnostic potential of laser-induced autofluorescence emission in brain tissue. J Korean Med Sci 12(2):135–142
5. Dailey HA, Smith A (1984) Differential interaction of porphyrins used in photoradiation therapy with ferrochelatase. Biochem J 223(2):441–445
6. Ishihara R, Katayama Y, Watanabe T et al (2007) Quantitative spectroscopic analysis of 5-aminolevulinic acid-induced protoporphyrin IX fluorescence intensity in diffusely infiltrating astrocytomas. Neurol Med Chir (Tokyo) 47(2):53–57
7. Toms SA, Lin WC, Weil RJ et al (2005) Intraoperative optical spectroscopy identifies infiltrating glioma margins with high sensitivity. Neurosurgery 57(4 Suppl):382–391
8. Lin WC, Toms SA, Johnson M et al (2001) In vivo brain tumor demarcation using optical spectroscopy. Photochem Photobiol 73(4):396–402
9. Savitzky A (1964) Smoothing and differentiation of data by simplified least squares procedures. Anal Chem 36(8):1627–1639
10. Wagnieres G (1998) In vivo fluorescence spectroscopy and imaging for oncological applications. Photochem Photobiol 68:603–632
11. Yin D (1996) Biochemical basis of lipofuscin, ceroid, and age pigment-like fluorophores. Free Radic Biol Med 21(6):871–888
12. Eldred GE, Miller GV, Stark WS et al (1982) Lipofuscin: resolution of discrepant fluorescence data. Science 216(4547):757–759
13. Zijlstra WG, Buursma A, van der Roest WPM (1991) Absorption spectra of human fetal and adult oxyhemoglobin,

de-oxyhemoglobin, carboxyhemoglobin, and methemoglobin. Clin Chem 37(9):1633–1638
14. Faber DJ, Mik EG, Aalders MCG et al (2003) Light absorption of (oxy-)hemoglobin assessed by spectroscopic optical coherence tomography. Opt Lett 28(16):1436–1438
15. Faber DJ, Aalders MCG, Mik EG et al (2004) Oxygen saturation-dependent absorption and scattering of blood. Phys Rev Lett 93(2):028102
16. Louis DN, Ohgaki H, Wiestler OD et al (2007) The 2007 WHO classification of tumours of the central nervous system. Acta Neuropathol 114(2):97–109
17. Utsuki S, Oka H, Sato S et al (2007) Histological examination of false positive tissue resection using 5-aminolevulinic acid-induced fluorescence guidance. Neurol Med Chir (Tokyo) 47(5):210–213
18. Janzer RC, Raff MC (1987) Astrocytes induce bloodbrain barrier properties in endothelial cells. Nature 325(6101):253–257
19. Janzer RC (1993) The blood-brain barrier: cellular basis. J Inherit Metab Dis 16(4):639–647
20. Noguchi M, Aoki E, Yoshida D, Kobayashi E, Omori S, Muragaki Y, Iseki H, Nakamura K, Sakuma I (2006) A novel robotic laser ablation system for precision neurosurgery with intraoperative 5-ALA-induced PpIX fluorescence detection. MICCAI 4190:543–550

Japanese Journal of Clinical Oncology Advance Access published April 12, 2013

JJCO Japanese Journal of Clinical Oncology

Jpn J Clin Oncol 2013
doi:10.1093/jjco/hyt051

Review Article

Drug Review: Safety and Efficacy of Bevacizumab for Glioblastoma and Other Brain Tumors

Yoshitaka Narita*

Department of Neurosurgery and Neuro-Oncology, National Cancer Center Hospital, Tokyo, Japan

*For reprints and all correspondence: Yoshitaka Narita, Department of Neurosurgery and Neuro-Oncology, National Cancer Center Hospital, 5-1-1, Tsukiji, Chuo-ku, Tokyo 104-0045, Japan. E-mail: yonarita@ncc.go.jp

Received January 21, 2013; accepted March 14, 2013

Glioblastoma is a highly vascular tumor that expresses vascular endothelial growth factor, a key regulator of angiogenesis and tumor blood vessel permeability. Bevacizumab is a monoclonal antibody that inhibits vascular endothelial growth factor and the growth of gliomas. Bevacizumab monotherapy has proven effective for recurrent glioblastoma, and it extended progression-free survival and improved patient quality of life in various clinical trials. Some patients who receive bevacizumab experience improvements in neurological symptoms and steroid dose reductions. Bevacizumab induces a dramatic and rapid radiological response, but non-enhancing lesions are often detected on magnetic resonance imaging without enhancing lesions. Rebound phenomena such as rapid tumor regrowth are occasionally observed after the discontinuation of bevacizumab therapy. Therefore, Response Assessment in Neuro-Oncology criteria were recently devised to evaluate the efficacy and radiological response of bevacizumab treatment. Hypertension and proteinuria are characteristic adverse events associated with bevacizumab therapy. In addition, many fatal adverse events such as intracranial hemorrhage and venous thromboembolism are reported in patients treated with bevacizumab. However, these events are also associated with glioma itself, and careful attention needs to be paid to these events. Bevacizumab is used to treat various diseases including radiation necrosis and recurrent brain tumors such as brain metastases, schwannoma and meningioma, but additional clinical trials are necessary. The efficacy and current problems associated with bevacizumab in the treatment of glioblastoma and other brain tumors are reviewed.

Key words: bevacizumab – glioblastoma – glioma – brain metastases – rebound

INTRODUCTION

Glioblastoma (GBM), the most common malignant brain tumor, is associated with a survival time of 1–2 years. The standard therapy for a newly diagnosed GBM is maximum resection in patients without neurological deficits and radiotherapy (RT) plus the alkylating agent temozolomide (TMZ) (1). GBM is a highly vascular tumor, and an alternative therapeutic approach that inhibits angiogenesis is expected to inhibit the growth of GBM.

Vascular endothelial growth factor (VEGF), a key regulator of angiogenesis, is highly expressed in GBM (2–4). The expression of VEGF correlates with the grade of gliomas (5), and VEGF expression is also observed in meningioma and brain metastases (3). The molecular bases for the upregulation of VEGF gene expression in gliomas are as follows: (i) hypoxia or the hypoxia inducible factor (HIF)-related mechanism, (ii) epidermal growth factor receptor signaling, (iii) upregulation of the Forkhead box M1B (FoxM1B) transcription factor in GBM but not in low-grade glioma, which stimulates VEGF expression independently of HIF and (iv) upregulation of HuR, a member of the Elav family of RNA-binding proteins, in GBM, which suppresses the post-

transcriptional degradation of VEGF mRNA under hypoxia (6). VEGF signaling regulates angiogenesis and tumor blood vessel permeability, which promote endothelial cell proliferation, survival and migration and cerebral edema (6).

Monoclonal antibodies against VEGF have been demonstrated to inhibit the growth of GBM xenografts in an *in vivo* mouse model (7,8). Bevacizumab (Avastin®), a monoclonal antibody that inhibits the VEGF, is currently approved for metastatic colorectal, non-small-cell lung, breast, ovarian and renal cancers. Based on the results of many clinical trials of bevacizumab for the treatment of GBM, bevacizumab is currently recognized as a second-line chemotherapeutic agent for GBM. The application of bevacizumab for recurrent GBM is also described in the National Comprehensive Cancer Network guideline (9), and it has been approved in more than 41 countries. This article reviews the efficacy and current problems of bevacizumab therapy against GBM and other brain tumors.

RECURRENT GBM

Bevacizumab is a standard therapeutic agent for recurrent GBM or WHO grade III malignant gliomas after treatment with RT plus TMZ, and no other effective therapy is available. Single-agent bevacizumab after the failure of initial treatment with mainly TMZ for malignant gliomas has a reported objective response rate (ORR), progression-free survival (PFS), 6-month PFS rate and overall survival (OS) of 20.9–42.6%, 1.0–4.2 months, 20.9–42.6% and 7.1–12 months, respectively, as calculated from the initiation of bevacizumab treatment (10–14) (Table 1).

Bevacizumab alone or in combination with irinotecan was similarly effective for recurrent GBM in the BRAIN study (11). The PFS times were 4.2 and 5.6 months in the bevacizumab alone ($n = 85$) and bevacizumab plus irinotecan ($n = 87$) groups, respectively, and the OS times were 9.2 and 8.7 months, respectively, in the two groups. The 6-month PFS rates for bevacizumab alone and bevacizumab plus irinotecan were 42.6 and 50.3%, respectively, and the ORRs were 28.2 and 37.8%, respectively, for the two treatments. Based on these results, the US Food and Drug Administration (FDA) first granted bevacizumab accelerated approval for the treatment of recurrent GBM in 2009 (15).

Table 1. Efficacy of single-agent bevacizumab for malignant gliomas

Study	ORR (%)	PFS	6-month PFS rate (%)	OS from bevacizumab
BRAIN, 2009	28.2	4.2	42.6	9.2
JO22506, 2012	27.6	3.3	33.9	10.5
Kreisl, 2009	35	3.7	29	7.1
Chamberlain, 2010	42	1.0	42	8.5
Kreisl, 2010	43	2.9	20.9	12

ORR; overall response rate, PFS; progression-free survival, OS; overall survival.

The JO22506 study in Japan also revealed that single-agent bevacizumab was effective for recurrent malignant gliomas ($n = 31$) (14). The PFS and OS were 3.3 and 10.5 months, respectively, for this treatment. Additionally, the 6-month PFS rate, ORR and disease control rate were 33.9, 27.6, and 79.3%, respectively, and these findings were comparable with those of the BRAIN study. Approximately 70% of patients who received corticosteroids before treatment were able to reduce their dose or discontinue corticosteroid therapy after bevacizumab treatment, and >70% of patients displayed a lower tumor volume on magnetic resonance imaging (MRI) 6 weeks after treatment in this study.

Combination therapy of bevacizumab and irinotecan (11,12,16–18), carboplatin (19–21), erlotinib (22), etoposide (23) and dose-intense daily TMZ (24,25) for malignant gliomas was reported, and the treatment results were similar to that of single-agent bevacizumab therapy.

Generally, the 6-month PFS rate and OS of recurrent GBM are 10–20% and ~6 months, respectively (26–28). Thus, single-agent bevacizumab has become the most promising second-line agent for recurrent GBM in adult. However, there are a few reports about the use of bevacizumab to treat recurrent pediatric high-grade gliomas or brainstem gliomas, and the radiological response rate, response duration and survival of children appeared to be inferior to those of adult cases (29–32).

Marked decreases in enhancing lesions and surrounding cerebral edema have been observed after the initiation of therapy, and patients exhibited improvements in clinical symptoms. Approximately 30–70% of patients who received bevacizumab could reduce their steroid doses (14,33). Steroids have been used to treat patients with brain tumors to control brain edema, and bevacizumab is occasionally considered an 'expensive super steroid'. Thus, patients treated with bevacizumab display improved quality of life due to improvements in clinical symptoms and reductions of steroid doses, even if for a short time.

Wong et al. performed a meta-analysis of bevacizumab for recurrent GBM in 548 patients from 15 studies and reported that the 6-month PFS rate and OS were 45% and 9.3 months, respectively. The treatment doses of bevacizumab in most clinical trials were 10 mg/kg every 2 weeks, but they reported no difference in the bevacizumab dose response benefit between doses of 5 mg/kg and 10–15 mg/kg (34). The efficacy of superselective intra-arterial cerebral infusion of bevacizumab to increase the local concentration of the drug around the tumor has been reported (35).

MRI FINDINGS AFTER BEVACIZUMAB TREATMENT

Bevacizumab exhibited a dramatic and rapid reducing effect on enhancing lesions on MRI (36,37), and >70% patients

displayed smaller enhancing lesions 6 weeks after the initiation of treatment (14). However, this effect is not caused by the antitumor effect of bevacizumab, but is attributable to the normalization of abnormally permeable tumor vessels or regional cerebral blood volume (38). Non-enhancing lesions on T2 or fluid-attenuated inversion recovery MRI are often detected without enhancing lesions, which are indicative of progressive infiltrative tumors. Iwamoto et al. reported that 46% of patients had larger enhancing lesions at the initial tumor site, 16% had a new enhancing lesion outside the initial site, and 35% had progression of predominantly non-enhancing tumors at the time of bevacizumab discontinuation for recurrent GBM (36).

The Macdonald criteria have been used for response assessment in glioma (39). These criteria are based on the two-dimensional WHO response criteria, and they use the enhancing tumor area on computed tomography (CT) or MRI as the primary measure while considering the use of steroids and changes in the neurologic status. However, these criteria cannot evaluate the enlargement of the non-enhancing area upon bevacizumab treatment or a pseudoresponse, which is often visualized as a transient increase in the enhancing lesion in patients receiving TMZ treatment. Thus, the Response Assessment in Neuro-Oncology Working Group developed new standardized response criteria for clinical trials of brain tumor treatment to evaluate the clinical response to recent treatment including antiangiogenic therapy (40).

REBOUND PHENOMENON AND BEVACIZUMAB CONTINUATION BEYOND PROGRESSION

No effective agent other than TMZ or bevacizumab is available to treat malignant gliomas, and TMZ or bevacizumab therapy, with or without other chemotherapeutic agents, often continues after progressive disease (PD) is observed. Increased doses of TMZ were reported to be beneficial for some patients (41–44). It is unclear whether continued bevacizumab treatment is effective in patients after PD is detected.

Two large observation studies showed that bevacizumab continuation beyond the initial diagnosis of PD improved the OS of patients with metastatic colorectal cancer (45,46). In the BRiTE study, patients with metastatic colorectal cancer receiving first-line bevacizumab with or without chemotherapy received further treatment after the first observation of PD as directed by a physician, and they were observed thereafter. The OS times beyond the first instance of PD for the no post-PD treatment ($n = 253$), post-PD treatment without bevacizumab ($n = 531$) and post-PD treatment with bevacizumab ($n = 642$) groups were 12.6, 19.9 and 31.8 months, respectively. Multivariate analyses demonstrated that the continuation of bevacizumab therapy was strongly and independently associated with improved survival after PD [hazard ratio (HR) = 0.48, $P < 0.001$] (45). Similar results were obtained in the ARIES study (46).

Reardon et al. analyzed the outcomes of patients who received subsequent therapy after PD to evaluate the efficacy of bevacizumab regimens against recurrent GBM in five studies (47). In the studies, bevacizumab was used in combination with irinotecan, daily TMZ, etoposide, bortezomib and erlotinib. The OS times of patients in the no post-PD treatment ($n = 41$), post-PD treatment without bevacizumab ($n = 44$) and post-PD treatment with bevacizumab ($n = 55$) groups were 1.5, 4.0 and 5.9 months, respectively (HR = 0.64, $P = 0.04$). The PFS times of patients in the post-PD treatment without bevacizumab ($n = 44$) and post-PD treatment with bevacizumab ($n = 55$) groups were 1.6 and 2.8 months, respectively (HR = 0.64, $P < 0.0001$). They concluded that bevacizumab continuation beyond the initial detection of PD modestly improves OS compared with available non-bevacizumab therapy for recurrent GBM.

Zuniga et al. (48) reported a rebound phenomenon after the discontinuation of bevacizumab in patients with malignant gliomas. Rebound PD was defined as an increase in the largest cross-sectional area of enhancement on MRI of at least 50% compared with that at the time of bevacizumab failure. Among 40 patients who did not respond to bevacizumab therapy, 11 patients (27.5%) displayed rebound PD, and they had poor prognoses with an OS of 6.8 weeks. Of three patients who were restarted on bevacizumab treatment after rebound PD, two exhibited a partial response, and the OS was extended to 21.3 weeks. Clark et al. (49) analyzed the survival of patients who underwent reoperation and reported that patients who received bevacizumab preoperatively had a worse postoperative OS (HR = 3.1, $P < 0.001$) and PFS than patients who did not receive bevacizumab.

Abrupt discontinuation of bevacizumab after PD may lead to a rebound phenomenon and increased tumor-associated cerebral edema, and therefore, continuation or slow tapering of the bevacizumab dose after PD might be necessary to prevent rebound PD.

NEWLY DIAGNOSED GBM

RT plus TMZ plus bevacizumab was applied for newly diagnosed GBM, and the OS and PFS times were 19.6–23 and 13–13.6 months, respectively (50,51). The efficacy of this combination therapy was superior to that of RT plus TMZ (OS = 14.6 months; PFS = 6.9 months) (1).

A Phase III trial of RT plus TMZ plus placebo vs. RT plus TMZ plus bevacizumab was conducted for 921 patients with newly diagnosed GBMs from 26 countries (52,53). The primary endpoints were PFS and OS, and the final PFS and interim OS results were presented at a Society of Neuro-Oncology meeting at the end of 2012. The PFS times of the placebo ($n = 463$) and bevacizumab groups ($n = 458$) were 4.3 and 8.4 months ($P < 0.0001$, HR = 0.61), respectively, and the addition of bevacizumab to RT plus TMZ significantly extended PFS. The median lengths of time for which patients maintained a Karnofsky performance status

score of ≥70 in the placebo and bevacizumab groups were 6 and 9 months, respectively. The bevacizumab group exhibited a significantly prolonged median duration of stability or improvement from baseline for health-related quality of life (HRQoL) as assessed by the EORTC QLQ-C30 and BN20 scores for global health status, physical functioning, social functioning, motor functioning and communication deficit compared with the placebo group. Considering that bevacizumab in addition to TMZ improves PFS and HRQoL in patients with newly diagnosed GBM, it is possible that RT plus TMZ plus bevacizumab will be a new standard therapy for a newly diagnosed GBM. The final results including OS will be presented in 2013.

BRAIN METASTASES

The standard therapy for brain metastases is RT or surgery plus RT depending on the size and number of tumors (54). The role of chemotherapy in the treatment of brain metastases has not been established. Because bevacizumab is believed to induce ICH in patients with brain metastases (55), patients with brain metastases have previously been excluded from clinical trials of bevacizumab. The PASSPORT study of patients with non-small lung cell carcinoma (NSCLC) and nonprogressive brain metastases after RT demonstrated that bevacizumab in addition to chemotherapeutic agents or erlotinib did not induce ≥grade 2 ICH and that bevacizumab can be safely used in patients with brain metastases (56).

A small series of patients with progressive brain metastases who failed on RT or surgery plus RT and received treatment with bevacizumab with or without chemotherapeutic agents were reported for breast cancer (57,58), NSCLC (59) and colorectal cancer (60). The ORR of the studies was 33–100%, and the PFS and OS of patients with breast cancer and brain metastases were 2.8–9 and 7.8 months, respectively. No ≥grade 2 ICH was reported in these studies. These studies were very small, but they suggest that bevacizumab can be effective in patients who fail to respond to RT. No effective chemotherapy for patients with radiation-naïve brain metastases is available, and further investigation of bevacizumab-based therapies is necessary.

SCHWANNOMA AND MENINGIOMA

Surgery is the first choice for WHO grade I benign brain tumors such as schwannomas and meningiomas, and no chemotherapeutic agent is available for these tumors. These benign tumors occasionally recur, and repeated surgery is necessary, resulting in the deterioration of patient health. Recent reports demonstrated that bevacizumab is effective against these tumors. Neurofibromatosis type 2 (NF2) is an autosomal-dominant syndrome characterized by bilateral vestibular schwannomas, meningiomas and gliomas. The effective treatment options include surgery and stereotactic radiosurgery, and these patients often lose hearing activity. Bevacizumab was reported to be effective for schwannomas in NF2 (61–65). Plotkin et al. reviewed 31 cases of vestibular schwannomas in NF2 and reported that the ORR was 55% and that 88% of patients had stable or decreased tumor size after 1 year (63). Ninety percent of patients had stable or improved hearing activity after 1 year of bevacizumab treatment, and hearing was stable or improved in 61% of patients after 3 years.

Most of meningiomas, the most common benign primary brain tumors, are WHO grade I, but some of them are aggressive WHO grade II or III malignant tumors. Some patients with WHO grade I meningioma in the skull base recur at the same tumor site, and repeated surgery or radiosurgery is often performed. The VEGF is highly expressed in meningiomas, and it plays a role in tumor angiogenesis and peritumoral edema (66). Bevacizumab with or without chemotherapeutic agents was reported to control recurrent meningioma (67–70). Lou et al. (68) reviewed 14 cases of grade I–III progressive/recurrent meningioma and reported that 1 patient had a partial response and 11 patients had stable disease, and the PFS was 17.9 months. In their study, bevacizumab was administered as a single agent to 4 patients, and 10 patients received bevacizumab with chemotherapy with etoposide or TMZ.

Bevacizumab is also reported to be effective for hemangiopericytoma and malignant solitary fibrous tumors that often arise in the brain and are highly angiogenic. Park et al. reviewed 14 patients with these tumors including 6 brain tumors who were treated with bevacizumab and TMZ and reported that the ORR and PFS were 79% and 9.7 months, respectively (71).

RADIATION NECROSIS AND RE-IRRADIATION THERAPY

Radiation necrosis is the most severe delayed toxicity associated with RT. The standard therapy for radiation necrosis includes steroids, anticoagulation and the removal of necrotic tissues. The pathophysiological mechanism of radiation necrosis is RT-induced endothelial dysfunction with elevated levels of cytokines such as VEGF, resulting in increased capillary permeability of the blood brain barrier, subsequent extracellular edema, loss of the myelin covering of neurons, and finally hypoxia and necrosis (72,73). Thus, the VEGF is a target in the treatment of radiation necrosis, and bevacizumab was demonstrated to be effective for radiation necrosis via restoration of the blood brain barrier (74–80).

A Phase III study of patients with radiation necrosis and progressive neurological symptoms was conducted (81). All patients who received bevacizumab treatment ($n = 7$) at a dose of 7.5 mg/kg every 3 weeks showed a decreased volume of radiation necrotic lesions on FLAIR and T1-weighted gadolinium-enhanced MRI and improved neurological symptoms at 6 weeks after treatment; however,

patients in the placebo group (saline treatment; $n = 7$) exhibited no improvements. Five (71%) patients in the placebo group experienced worsening of neurological symptoms, and the other two patients showed progression on MRI. Bevacizumab at a dose of 7.5 mg/kg every 3 weeks for 12 weeks can stop the progression of radiation necrosis in most patients for least at 10 months after treatment. Levin et al. concluded that the study provided class I evidence for the efficacy of bevacizumab in the treatment of radiation necrosis secondary to the treatment of head-and-neck cancer and brain tumor.

Approximately 80% of patients with GBM have local recurrence at the original tumor site (82,83), and re-irradiation is a salvage treatment option, although it is limited by the radiation tolerance of surrounding normal brain tissue. Re-irradiation with hypofractionated stereotactic RT (HFSRT) at a dose of 20–36 Gy appears to be effective with acceptable toxicity (84–88). The OS after re-irradiation was reported to range between 3 and 10 months. Because bevacizumab is effective for recurrent high-grade gliomas and reduces the toxicity associated with RT, re-irradiation with HFSRT or radiosurgery combined with bevacizumab has been attempted for recurrent high-grade gliomas (88–90). OS after re-irradiation was reported to be 7.2–18 months in this series, compared with 3.3–12 months in the absence of bevacizumab as per historical data. Re-irradiation with bevacizumab is a promising therapeutic option, but further randomized clinical trials are needed.

ADVERSE EVENTS

Major adverse events associated with treatment with bevacizumab alone for recurrent gliomas include hypertension (HT), ICH, venous thromboembolism (VTE), proteinuria, and wound-healing complications, and the proportions of these events that were all grades/≥grade 3 (according to the National Cancer Institute Common Terminology Criteria for Adverse Events version 3.0: NCI-CTCAE) were 12.6–35.7%/4.2–16% (HT), 0–3%/0% (ICH), 3.2–16.0%/2.0–12.6% (VTE), 2.1–41.9%/0–3.2% (proteinuria), and 0–6.0%/0–2.4% (wound-healing complications), respectively (10–14) (Table 2). The rates of various types of hemorrhage including ICH, epistaxis, gingival bleeding, conjunctival hemorrhage and infusion site hemorrhage and the presence of blood urine were reported to range as high as 30% in previous studies (11,14). Arterial thromboembolism was also reported (11), but gastrointestinal perforation is a rare complication in the treatment for gliomas (10–14).

HT, the most common adverse event in patients treated with bevacizumab, is a cause of ICH, cerebral ischemia, and myocardial infarction. A recent meta-analysis revealed that the incidences of all-grade and grade 3–4 HT in patients receiving bevacizumab were 23.6 and 7.9%, respectively, and that the relative risk (RR) of high-grade HT is 5.3 ($P < 0.001$) (91). The mechanisms of bevacizumab-induced HT

Table 2. Major adverse events of single-agent bevacizumab for malignant gliomas (% All grades/% ≥grade 3)

Study	BRAIN, 2009	JO22506, 2012	Kreisl, 2009	Kreisl, 2010	Chamberlain, 2010
Number of patients	85	31	48	31	50
Hypertension	35.7/8.3	32.3/9.7	12.6/4.2	32.0/16.0	14.0/6.0
Intracranial hemorrhage	2.4/0	3.2/0	0/0	0/0	4.0/0
Venous thromboembolic events	3.6/3.6	3.2/3.2	12.6/12.6	6.4/6.4	8.0/2.0
Proteinuria	4.8/0	41.9/0	2.1/0	28.8/3.2	10.0/2.0
Wound-healing complications	6.0/2.4	0/0	0/0	3.2/0	4.0/2.0
Gastrointestinal perforation	0/0	0/0	2.1/2.1	0/0	0/0

are renal thrombotic microangiopathy, glomerular damage, and vascular effects. Bevacizumab decreases the production of nitric oxide in the wall of arterioles, which induces endothelial dysfunction and increases systemic vascular resistance (92). Several reports suggest that very early HT is associated with the tumor response to bevacizumab in patients with colorectal cancer and non-small lung carcinoma (93,94), but Wick et al. reported that there was no prognostic correlation between HT and bevacizumab treatment in patients with GBM (95).

Proteinuria is a characteristic adverse event of VEGF inhibitors that may lead to renal failure, HT, and cardiovascular complications. One of the mechanisms of proteinuria is the injury of glomerular endothelium due to VEGF inhibition mediated by bevacizumab (96). A recent meta-analysis revealed that the incidence of grade 3–4 proteinuria in patients treated with bevacizumab was 2.2%, and its RR was 4.8 (97). High-dose ($5.0\ mg{\cdot}kg^{-1}week^{-1}$) and low-dose ($2.5\ mg{\cdot}kg^{-1}week^{-1}$) bevacizumab treatment is associated with increased risk of proteinuria, with RRs of 2.2 and 1.4, respectively (98). Close monitoring of blood pressure, blood pressure examination and urine tests are necessary because patients who require dialysis or who have been diagnosed with persistent nephrotic syndrome even after bevacizumab discontinuation were reported. When grade 3–4 proteinuria is observed, the dose of bevacizumab should be reduced or discontinued.

ICH can be a life-threatening event for patients with malignant brain tumors. ICH occurs primarily via intratumoral bleeding. Velander reviewed the incidence of ICH in patients with cancer and reported that its incidence is as high as 10% (99). ICH occurs in all cancers, and GBM, oligodendroglial tumors, lung cancer, breast cancer, melanoma, renal cell carcinoma, hepatocellular carcinoma, choriocarcinoma and thyroid cancer are the common malignancies in which ICH occurs as part of the natural history of the lesion. Since the

occurrence of fatal ICH in a patient in an early phase I study of hepatocellular carcinoma, bevacizumab has been contraindicated in Japan and Europe for use in patients with brain metastases from systemic cancers. Besse et al. analyzed the incidence of ICH in various clinical studies and reported that its incidence was 0.8–3.3 or 1.0% in patients with brain cancer who were treated with bevacizumab or were not treated with bevacizumab, respectively (100). Khasraw et al. (101) also reported that there was no difference in the incidence of ICH between patients with malignant brain tumors including GBM and brain metastases receiving bevacizumab (3.7%) and those not receiving bevacizumab (3.6%). Based on these findings, bevacizumab does not appear to increase the incidence of ICH compared with its natural incidence in gliomas or brain metastases, and bevacizumab is not contraindicated for malignant brain tumors.

Bevacizumab is reported to increase the risk of arterial thromboembolic events including myocardial infarction and angina with an RR of 2.1 (102) or a HR of 2.0 (103). Whether it increases the risk of cerebral stroke is controversial (102). Cerebral stroke is often observed in patients with brain tumors. Kreisl et al. reported that the majority of strokes are caused by surgery or RT and that the median latency from RT to stroke was 3.2 years (104). Fraum et al. reported that ischemic stroke occurred in 1.9 and 1.7% of patients who were treated with and without bevacizumab, respectively (105).

Patients treated with bevacizumab were reported to have a significantly increased risk of VTE with an RR of 1.3 compared with controls, and the risk was not different between patients receiving bevacizumab doses of 2.5 and 5.0 $mg{\cdot}kg^{-1}week^{-1}$ (106). However, GBM and malignant gliomas themselves are risk factors for VTE. The 2-year cumulative incidence of VTE was reported to be 7.5% in patients with malignant gliomas, and 55% of these patients were diagnosed within 2 months after surgery (107). Risk factors for VTE include older age (HR = 2.6), GBM histology (HR = 1.7), and chronic comorbidities (HR = 3.5) (107). Another study showed that the cumulative incidence of VTE was 21% at 3 months and 26% at 12 months after surgery and that residual tumors represented a risk factor (HR = 3.6) (108). Thus, VTE is often observed in patients with malignant glioma; however, and importantly, anticoagulation does not appear to increase the risk of ICH, and therapeutic anticoagulation for patients with malignant brain tumors and arterial or venous thromboembolism should be recommended (99). Treatment with bevacizumab concomitant with anticoagulation for VTE possibly increases the risk of ICH; however, these treatments did not necessarily cause severe hemorrhages with clinical symptoms, and patients treated with bevacizumab should be given low-molecular-weight heparin or warfarin with close monitoring of blood test examination whenever needed (109,110).

Posterior reversible encephalopathy syndrome (PRES) is a syndrome clinically characterized by HT, headache, confusion, visual disturbances and seizures. The causes of PRES are severe HT, eclampsia, cerebrovascular events, immunosuppressive agents and chemotherapeutic agents, and PRES was reported as an adverse effect of bevacizumab in the treatment of systemic cancers (111–113). Most patients who develop PRES during bevacizumab treatment had an increase in blood pressure from baseline, and PRES resolved after prompt withdrawal of bevacizumab and normalized control of blood pressure (113).

VEGF plays an important role in the healing of surgical wounds, and the preoperative and postoperative use of bevacizumab may increase the risk of wound-healing complications. Because the half-life of bevacizumab is approximately 3 weeks (20 days), patients should wait at least 6–8 weeks to have surgery after the cessation of bevacizumab treatment (114). Postoperative initiation of bevacizumab should be delayed by 4 weeks to prevent an increased risk of wound-healing complications. Clark et al. (115) analyzed 209 patients who underwent a second or third craniotomy and showed that patients receiving preoperative bevacizumab therapy developed wound-healing complications more commonly than those not receiving bevacizumab therapy (35 vs. 10.0%, $P = 0.004$). Patients with an interval of <28 days between the last dose of bevacizumab and surgery tended to have an increased risk of this complication compared with those with an interval of ≥28 days (odds ratio = 6.5, $P = 0.07$), albeit without significance. In total, 1 of 18 patients (6%) with a median of 43 days (range 22–65 days) between surgery and postoperative bevacizumab initiation had wound-healing complications, a rate that was not significantly different from that for controls not receiving bevacizumab treatment. The authors recommend performing repeated craniotomy more than 28 days after the last administered dose of bevacizumab whenever possible.

CONCLUSIONS

Single-agent bevacizumab is effective for recurrent GBM and improves the quality of life of patients. HT and proteinuria are characteristic adverse events associated with bevacizumab treatment. Many fatal adverse events such as ICH and VTE are reported in patients with gliomas. However, these events are also associated with glioma itself, and these events should receive due attention. Bevacizumab is used to treat various diseases including brain tumors and radiation necrosis, but further clinical trials are necessary.

Conflict of interest statement

None declared.

References

1. Stupp R, Mason WP, van den Bent MJ, et al. Radiotherapy plus concomitant and adjuvant temozolomide for glioblastoma. *N Engl J Med* 2005;352:987–96.